ELSEVIER

Inorganica Chimica Acta 226 (1994) 187–194

Inorganica Chimica Acta

A spectroelectrochemical method for evaluating factors which regulate the redox potential of hemoglobins

Kevin M. Faulkner [a], Celia Bonaventura [b], Alvin L. Crumbliss [a,*]

[a] *Department of Chemistry, Duke University, Durham, NC 27708-0346, USA*

[b] *School of the Environment Marine Laboratory, Duke University, Beaufort, NC 28516-9721, USA*

Received 11 April 1994

Abstract

Spectroelectrochemical techniques were used to evaluate the redox potential of various hemoglobins under various experimental conditions. We use $Ru(NH_3)_6^{3+}$ as a redox mediator, which exchanges electrons with heme iron through an outer-sphere mechanism. Use of this mediator offers the advantage that it does not act as an allosteric effector. Studies of Hb stabilized in varied conformations confirm previous reports that Hb in the high oxygen affinity (R state) conformation is typically more easily oxidized than in the low oxygen affinity (T state) conformation. Accordingly, Nernst plots for Hb show evidence of cooperativity, with redox potentials that are sensitive to T state stabilization by anionic effectors. Alterations of the redox potential that are independent of the protein's conformational equilibrium between R and T states are exemplified by imidazole interactions with Hb. Imidazole binds preferentially to metHb. Changes in the redox potential induced by imidazole are very different from the changes associated with binding of heterotropic anionic effectors. Effectors such as inositol hexaphosphate stabilize the T state, significantly lower cooperativity of the oxidation process, and reduce the ease of oxidation. In contrast, as the imidazole concentration is increased, Hb is more readily oxidized, and cooperativity is maintained. These marked differences make it possible to use spectroelectrochemistry to differentiate between redox changes brought about by conformational shifts and changes brought about by other alterations in the active site.

Keywords: Spectroelectrochemistry; Redox potentials; Hemoglobins; Ruthenium amine complexes; Cooperativity

1. Introduction

The cooperative behavior of vertebrate hemoglobin is a classic example of active-site regulation of proteins by environmental factors [1]. In spite of many insights gained from the study of structure/function relationships in various forms of hemoglobin and myoglobin, the factors responsible for regulating oxygen affinity are still not fully understood [2]. Steric and electronic aspects are clearly involved in the molecular controls of hemoglobin function. Steric interactions are exemplified by the interaction of active-site ligands with amino acid residues in the heme pocket [2–6]. Oxygen entry into the heme pocket is thought to be sterically hindered by interactions with Val E11β, while in some stereochemical conditions the bound oxygen can form hydrogen bonds to His E7 that stabilize the liganded state [2–6]. Electronic interactions directly or indirectly alter the electron density at the heme iron. Such interactions are exemplified by the displacement of the Fe from the porphyrin ring as a result of ligand-linked conformational changes. Displacement results in changes within the inner-coordination sphere of the Fe. Electron density alterations are associated with changes in the distances between Fe and the ϵ-nitrogen of the proximal histidine, His F8, and between Fe and the pyrole nitrogens of the heme ring [3,4].

Cooperativity refers to the positive interaction of active sites within an oligomeric system such that the activity of one site is influenced by the activity of another site through structural changes in the oligomer [7]. The 23–31 Å separation between active sites (Fe porphyrins) in Hb precludes the direct interaction of one Fe porphyrin with another [8]. The challenge then is to explain how distant sites can interact with one another. This prompted the formulation by Monod, Wyman, and Changcux of a model (the MWC model) that explains cooperativity in terms of an equilibrium between two conformational states [7]. Due to its conceptual elegance, the MWC model is frequently

* Corresponding author.

SSDI 0020-1693(94)04086-B

used to describe cooperativity in Hb and other systems of biological interest, with extensions sometimes added to allow for system complexity [1].

The deoxyHb ↔ metHb equilibrium is altered by homotropic and heterotropic allosteric effects. Homotropic effects are indicated by cooperative Nernst plots, where the oxidation state of one active site in the Hb tetramer impacts the redox potential of other active sites as a result of shifts in quaternary conformation. Heterotropic effects arise from conformational shifts that affect the active site as a result of the binding of effectors at sites other than the active site. In terms of a simple two-state model, both homotropic and heterotropic allosteric effects can be considered to influence the inner-coordination sphere of the Fe porphyrin and its redox potential as a result of altering the quaternary conformational equilibrium.

Spectroelectrochemistry offers the possibility of examining electronic interactions exclusive of the steric interactions in hemoglobins. Accordingly, we have undertaken a study of the electron transfer process in various hemoglobins to elucidate the specific influence of electronic effects on cooperativity in the hemoglobins [9]. This manuscript presents spectroelectrochemical results that allow simultaneous attainment of redox equilibrium and spectral characterization in the visible and UV regions. Oxygen, an active site ligand which can act as an oxidant, is eliminated from the system, and our mediator, hexammineruthenium(II/III), is not an allosteric effector. Thus, we are able to evaluate both homotropic effects and heterotropic effects more readily than in previous studies of hemoglobin redox chemistry [10].

As will be shown, the redox potential of Hb can be altered by mechanisms other than the homotropic and heterotropic effects described by the MWC model. It is possible to perturb the inner-coordination sphere directly, exclusive of directly influencing the R ↔ T equilibrium. This mechanism of altering the redox potential is illustrated herein by addition of imidazole to the system. We chose imidazole as an interactive active-site ligand because it has a highly preferential binding to the met form of Hb [10]. Previous studies showed that imidazole can greatly decrease the redox potential of Mb, where knowledge of the dissociation constant for met(ferri)myoglobin of $K_o = 8 \times 10^{-3}$ M allowed estimation of the dissociation constant for ferromyoglobin, with a K_r of about 1.5 M [10]. Imidazole is a strong field ligand which shifts the equilibrium spin state of Fe(III) from high-spin $Fe(III)OH_2$ to the low-spin Fe(III)imid complex [11,12], a situation which models the spin transition from high-spin deoxyHb to low-spin oxyHb.

The MWC model [7] is thus used successfully in this paper to describe aspects of the spectroelectrochemistry of Hb that are sensitive to the quaternary equilibrium between R and T states, while the imidazole effects observed do not fit within the framework of the MWC model.

2. Experimental

2.1. Materials

$Ru(NH_3)_6Cl_3$ (Strem Chemical Co. >99%), $NaNO_3$ (Fisher Scientific >99%), KCl (Fisher Scientific >99%), imidazole (Calbiochem >95%), MOPS (3-[*N*-morpholino]propanesulfonic acid) (Sigma Chemical Co. >99%), IHP (myo-inositol hexakis[dihydrogen phosphate] dipotassium salt) (Sigma Chemical Co. >95%), myoglobin (lyophilized solid from horse skeletal muscle, Sigma Chemical Co. >96%) and Pt (52 mesh gauze, Fisher Scientific 99.95%) were used as obtained. Doubly distilled water was used in all experiments.

Samples of chromatographically purified human hemoglobin A_0 (HbA_0) and carboxypeptidase-digested hemoglobin (HbCPA) were prepared by standard methods [13]. Samples were stripped of organic phosphates prior to chromatographic purification. Sample concentration and compositions were determined spectrophotometrically as described in the literature [14]. The amounts of oxidized Hb (metHb), oxygenated Hb (oxyHb), and hemichrome were determined by the spectral analysis. Samples that contained measurable amounts of hemichrome were discarded. The final concentration of the stock Hb solution was typically 1–2 mM in heme units. Hb was stored after preparation in liquid nitrogen or at +4 °C until further use.

2.1.1. Preparation of samples: Hb, buffer, mediator, and allosteric effectors

The electrochemical mediator, $Ru(NH_3)_6Cl_3$, was dissolved to give a concentration of 3–5 mM in the desired buffer/electrolyte solution. MOPS buffer was used due to its non-complexing nature and stability. Trizma buffers are unsatisfactory in that the system is slow to come to equilibrium and they cause an increase in the rate of hydrolysis of $Ru(NH_3)_6Cl_3$. The mediator/buffer solutions were stored under argon at 4 °C. For a given experiment, a desired amount of mediator solution was added quantitatively to about 500–700 μl of the proper buffer/electrolyte in a 5 ml flask and connected to a vacuum line for repeated pump-purging with Ar, followed by the addition of Hb and additional pump-purging with gentle swirling to minimize bubbling. Final concentrations were typically 0.35–1.0 mM in $Ru(NH_3)_6Cl_3$, and 0.050–0.20 mM in heme.

Stock solutions of inositol hexaphosphate (IHP) were prepared by dissolving a weighed amount of the solid into the desired buffer/electrolyte solution, followed by addition of 1 N NaOH and dilution to the desired

volume and pH. For experiments where IHP or other phosphates were required, additions were made to the mediator/buffer solution from the concentrated stock solution prior to the addition of stock Hb solution. The IHP concentration was 10-fold over the Hb (tetramer) unless otherwise noted.

2.2. Methods

2.2.1. Spectroelectrochemistry

The anaerobic optically transparent thin layer electrochemical cell (OTTLE) consists of a 1 cm×2 cm piece of 52 mesh Pt gauze placed between the inside wall of a 1 cm path length cuvette and a piece of silica glass held in place with a Tygon spacer. This arrangement results in an optical path length of about 0.055 cm, as calculated from the absorbance of Hb at 555 nm, $\epsilon_{555} = 12\,500\,M^{-1}\,cm^{-1}$ [10]. An air-tight seal was formed at the top of the cell with a rubber septum (Aldrich), through which protruded a connecting Pt wire to the working Pt gauze electrode and a Pasteur pipette salt bridge plugged at the end with agar for the Ag/AgCl reference (BAS) and Pt auxiliary (when used) electrodes. The salt bridges were filled with supporting electrolyte purged with Ar, which was passed through a Chromopack oxygen scavenger. The OTTLE was purged with Ar for 15 min prior to injecting protein samples. Hb remains in the deoxyHb state at open circuit for at least 4 h without mediator, and 6–8 h with mediator at closed circuit.

In a typical experiment about 500 μl of Hb/mediator solution were transferred via gas-tight syringe to the Ar purged OTTLE. The OTTLE cell was placed in a temperature controlled cell holder in the sample compartment of a CARY 2300 UV–Vis–NIR spectrophotometer. Potential control of the three-electrode system was achieved using a PAR model 175 potentiostat in conjunction with a PAR model 173 programmer for cyclic voltammetry studies of $Ru(NH_3)_6Cl_3$. All potentials are quoted relative to the Ag/AgCl electrode. $E_{1/2}$ of the $Ru(NH_3)_6^{3+/2+}$ is −150 mV at a Pt button electrode and in the OTTLE cell containing 0.05 M MOPS, 0.20 M KCl, pH 7.15.

Spectroelectrochemistry was carried out at a single wavelength, typically one of the protein Soret bands (430 nm, $\epsilon = 1.33\times10^5\ M^{-1}\,cm^{-1}$ for deoxyHb and 406 nm, $\epsilon = 1.62\times10^5\ M^{-1}\,cm^{-1}$ for ferric(met)Hb) [10]. The potential of the working electrode was held at +200 mV to oxidize all Hb to metHb. The absorbance was then set at zero. Next, the potential was jumped to some reducing potential where the amount of reduced material was about 5% (typically +20 to 0.0 mV), and held until the absorbance ceased to change (typically 5 to 15 min). Potential jumps went from oxidizing to reducing potentials in 10 to 20 mV increments. The final potential jump was made from a potential where ~95% of the material was reduced (−160 to −200 mV), to −450 mV. At this extreme negative potential all material is in the reduced state. The absorbance at −450 mV is taken as the total absorbance (A_{Tr}) of the Hb in the deoxyHb state. The spectroelectrochemical process can also be carried out in the oxidative direction. In this case the initial potential was −450 mV. Next, the potential was taken to ~−200 mV and the procedure continued in reverse from that described for the reductive direction. Fig. 1 illustrates a series of spectra taken from 750 to 370 nm during the stepwise oxidation process as described above. At our conditions and using $Ru(NH_3)_6Cl_3$ as a mediator, the redox process is chemically reversible for HbA_0 in the oxidative and reductive directions. This was apparent by the relative rates of oxidation and reduction of Hb in a given experiment, and by the superposition of Nernst plots obtained by oxidative and reductive potential changes. The rate of oxidation of Hb was slower than the rate of reduction, but still rapid on the time scale of an experiment. Total reduction of metHb in a single step takes about 10 min while total oxidation of deoxyHb in a single step takes about 20 min.

2.2.2. Spectroelectrochemistry of well-defined systems

Our spectroelectrochemical technique was tested on three thoroughly studied redox systems: 2,6-dichlorophenolindophenol (DCPIP), methylene blue and horse myoglobin (hMb). For hMb we have established by coulometry that the total number of electrons transferred (n) is 1. Literature reports of coulometric experiments on DCPIP and methylene blue establish $n = 2$

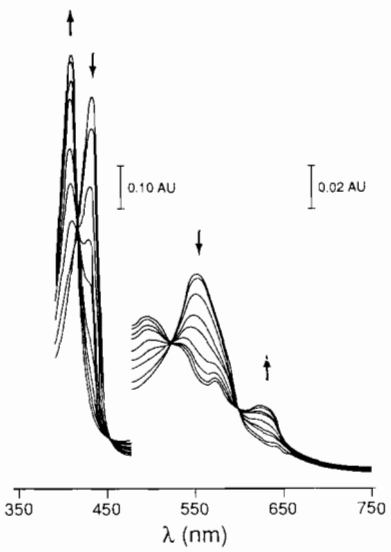

Fig. 1. Spectral changes observed from 750 to 370 nm during stages of HbA_0 oxidation. The initial spectrum is of deoxyHb, which has absorbance maxima at 430 and 555 nm. These absorbances decrease as the potential of the electrode is jumped to +200 mV, while absorbances at 404 and 630 nm increase. The 404 and 630 nm bands are characteristic of metHb. Optical path length = 0.055 cm.

for these systems [15]. Our spectroelectrochemical results for DCPIP, methylene blue and hMb are in excellent agreement with literature data. Ideal Nernstian behavior as defined by Heineman was observed with our spectroelectrochemical method for these simple redox systems [16]. We conclude that the spectroelectrochemical method employed in this work is a valid procedure for obtaining parameters related to the electron transfer properties of light-absorbing molecules.

2.2.3. Data analysis

The absorbances of the Hb Soret band at various potential values were converted to a ratio of [oxidized form]/[reduced form] by using Eq. (1), where $A_{Tr(430)}$ is the absorbance at 430 nm when the potential of the working electrode was −450 mV and Hb was totally reduced, and A_{E430} is the absorbance at 430 nm at each potential E.

$$[\text{oxidized form}]/[\text{reduced form}] = (A_{Tr(430)} - A_{E430})/A_{E430} \quad (1)$$

The log of this ratio plotted as a function of potential constitutes a Nernst plot as expressed in Eq. (2)

$$\log[\text{oxid.}]/[\text{red.}] = (n/58.1)E - (n/58.1)E^\circ \quad (2)$$

where E is the potential of the working Pt gauze electrode controlled by the potentiostat, E° is the reduction potential ($\log[\text{oxid.}]/[\text{red.}] = 0$), n is the slope, and 58.1 is the value of RT/F at 20 °C. For a complex multi-centered redox system, the formal redox potential, $E^{\circ\prime}$, is difficult to define. Therefore, we define the E° value as the value of E at half-oxidation, as is done for the case of non-ideal Nernstian behavior [16]. For a non-interactive system, the Nernst plot will be linear and the slope n is indicative of the number of electrons transferred. Thus n would be expected to be unity for Mb and 2 for DCPIP. The complex nature of a multi-centered redox system such as described here precludes the determination of electron stoichiometry. For an interactive multi-centered redox system the Nernst plot will not be linear and the slope n, which is not constant, will be indicative of that interaction and therefore will not correspond to the number of electrons transferred [16]. Thus the n parameter, as obtained from the slope of Eq. (2), may be interpreted in a similar manner to the n parameter one obtains as the slope of a Hill plot of O_2 binding data for systems with interactive active sites, where n values greater than 1 are an indication of cooperative interactions.

The spectroelectrochemical data were plotted according to Eq. (2) using a curve-fitting program ('Prostat' Ward and Reeves, IBM Version) which allows a first derivative plot of the fitted curve to be taken. Due to the precision in our results, we are able to define two n values. The n_{50} value is the slope of the Nernst plot at E°. Often, the maximum value of the slope, n_{max}, was found at potentials greater than the E° value, thus giving rise to a parameter we define as ΔE_n (the potential at the maximum n value minus E°; $En_{max} - E^\circ$) [9]. ΔE_n is dependent on experimental conditions and is used to describe the asymmetry induced in the Nernst plot. The E° and En_{max} values are related to the $\alpha_{1/2}$ and α_{max} values described in the two-state model for O_2 binding [17].

Experiments reported herein were reproduced at least twice and the reproducibility of the various spectroelectrochemical parameters at different buffer and background electrolyte conditions is as follows: in 0.05 M MOPS, $E^\circ = \pm 3$ mV, $n = \pm 0.10$ units; in 0.05 M MOPS, 0.20 M KCl, MOPS/KCl salt-bridge, $E^\circ = \pm 2$ mV, $n = \pm 0.10$ units; in 0.05 M MOPS, 0.20 M $NaNO_3$, saturated $NaNO_3$ in salt-bridge, $E^\circ = \pm 1$ mV, $n = \pm 0.05$ units.

3. Results

Hexammineruthenium(III/II) ($Ru(NH_3)_6^{3+/2+}$), the cationic mediator used in our electrochemical studies, was selected for use because its redox potential is in the correct range and because hemoglobin function is relatively insensitive to cations. The mediator's positive charge precludes interaction with the anion binding sites of hemoglobin. Our results (E°, n_{50}, n_{max}, ΔE_n) are independent of the $Ru(NH_3)_6^{3+/2+}$ concentration and the $[Ru(NH_3)_6^{3+/2+}]$/[heme] ratio, both in the presence and absence of nitrate anion, a known allosteric effector. For example, the parameters obtained for HbA_o in row 2 of Table 1 (the absence of $NaNO_3$ background electrolyte) were obtained without variation over a range of $[Ru(NH_3)_6Cl_3]$ from 0.47 to 1.57 mM at a [heme] of 0.166 mM. The parameters obtained for HbA_o in row 3 of Table 1 (in the presence of 200 mM $NaNO_3$ background electrolyte) were obtained without variation over a range of $[Ru(NH_3)_6Cl_3]$ from 0.23 to 1.19 mM at a [heme] range from 0.106 to 0.404 mM. Variations in the Cl^- counterion, also a known Hb allosteric effector, did not influence our results at these concentration ranges and conditions.

HbA_0, in the absence of allosteric effectors, exists in a R ↔ T equilibrium and undergoes a transition from the T state to the R state on oxidation to the met form, or on reaction with oxygen to form oxyhemoglobin. We use HbCPA as our model for a Hb stabilized in the R state and HbA_0 in the presence of an excess of the allosteric effector IHP as our model for T state stabilized Hb. A Nernst plot for all three of these systems is shown in Fig. 2. As expected, the E° value for HbA_0, illustrated in Fig. 2 and listed in Table 1, is intermediate between that for HbCPA and HbA_0/

Table 1
Spectroelectrochemical data for HbCPA and HbA_0 in the presence[a] and absence[b] of imidazole

Protein	Buffer	Cofactor	[Imid.] (mM)	[Imid.]/[heme]	$E°$ (mV)	n_{50}	n_{max}	ΔE_n (mV)
HbCPA	0.05 M MOPS	0.2 M $NaNO_3$	0	0	−155	1.0	1.0	0
HbA_0	0.05 M MOPS		0	0	−104	2.0	2.1	0
HbA_0	0.05 M MOPS	0.2 M $NaNO_3$	0	0	−63	1.5	1.7	30
HbA_0	0.05 M MOPS	0.2 M $NaNO_3$ Hb:IHP = 1:10	0	0	−40	1.0	1.2	>100
HbA_0	0.05 M MOPS	0.2 M $NaNO_3$	0.820	4:1	−77	1.3	1.6	30
HbA_0	0.05 M MOPS	0.2 M $NaNO_3$	10.4	48:1	−95	1.7	2.1	15
HbA_0	0.05 M MOPS	0.2 M $NaNO_3$	23.2	125:1	−123	1.7	2.2	23
HbA_0	0.05 M MOPS	0.2 M $NaNO_3$	52.3	218:1	−150	1.9	2.3	20
HbA_0	0.05 M MOPS	0.2 M $NaNO_3$	104	435:1	−170	2.2	2.4	15

[a]Conditions: pH = 7.1; 20 °C; potentials vs. Ag/AgCl; a saturated $NaNO_3$ reference electrode salt-bridge was used for data obtained in the absence of imidazole; $[Ru(NH_3)_6Cl_3]$ = 0.30–1.1 mM; [heme] = 0.1–0.23 mM.
[b]Data collected as in a; see Ref. [9].

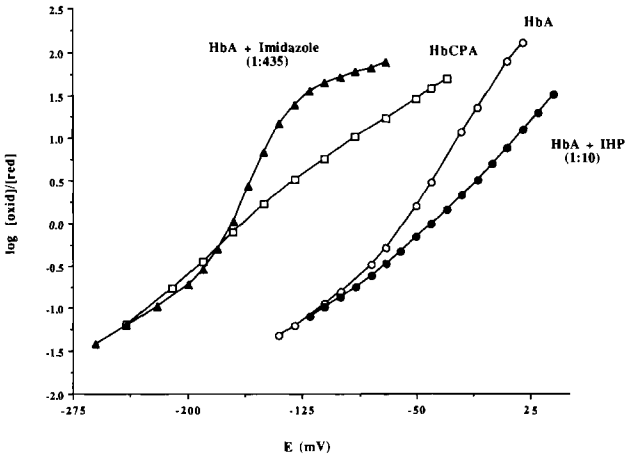

Fig. 2. Nernst plots for HbCPA and HbA_0, and HbA_0 in the presence of excess IHP and in the presence of excess imidazole. Conditions are as described in Table 1.

IHP. Stabilization of the R state produces a higher oxygen affinity protein which is more easily oxidized (i.e. has a more negative $E°$). Stabilization of the T state by the addition of IHP decreases the oxygen affinity and makes the iron centers more difficult to oxidize, as illustrated by the shift in $E°$ to a more positive value. The redox potentials and n values for the Nernst plots in Fig. 2 are included in Table 1.

The shape of the Nernst plots in Fig. 2 and the n values listed in Table 1 are indicative of cooperativity in electron transfer for these hemoglobins. Of the three proteins under discussion in Fig. 2, HbA_0 in the absence of an allosteric effector exhibits the greatest degree of cooperativity. HbCPA is essentially a non-cooperative protein. Cooperativity is reduced in HbA_0/IHP by shifting the R↔T equilibrium to the T state, which is consistent with the model we use to describe the cooperativity of Hb electron transfer. Stabilization of the T state is also indicated by the large ΔE_n value [9] for Hb/IHP listed in Table 1. Table 1 also includes data for HbA_0 in the presence of 200 mM NO_3^-. These results are consistent with NO_3^- acting as an allosteric effector which is weaker than IHP. The $E°$ is shifted positive relative to HbA_0 and the n values are diminished, consistent with a stabilization of the T state by NO_3^- binding at the protein anion site.

Table 1 and Fig. 3 illustrate the results of our spectroelectrochemical experiments for HbA_0 in the presence of varying concentrations of imidazole. The $E°$ values become increasingly negative as the imidazole concentration increases, consistent with the strong preferential binding to the ferric state over the ferrous state reported for Mb [10]. Fig. 2 includes a Nernst plot for HbA_0 in the presence of excess imidazole. Cooperativity in electron transfer is maintained, showing that neither the R nor the T states are strongly stabilized by imidazole addition. The ΔE_n values are similar to ΔE_n values for HbA_0 in 0.20 M NO_3^-, pH 7.1 (Table 1, row 3) and remain relatively constant. The inset in Fig. 3 shows a plot of n_{max} as a function of [imidazole].

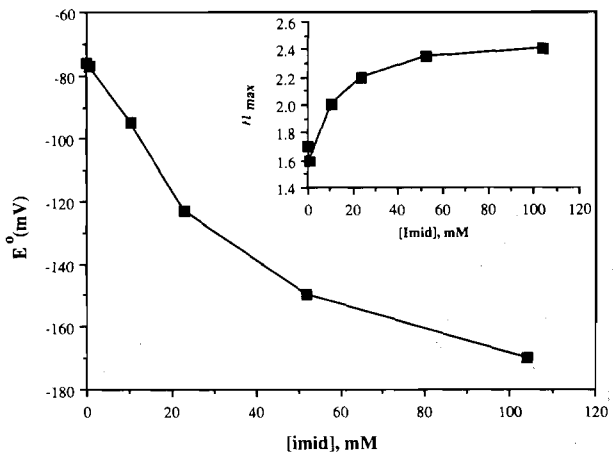

Fig. 3. Plot of $E°$ (vs. Ag/AgCl) as a function of imidazole concentration for HbA_0. Inset: Plot of n_{max} as a function of imidazole concentration. Conditions are as described in Table 1.

The data in Fig. 3 show a regular trend in $E°$ and n_{max} as the [imidazole] is increased. These data are consistent with a single imidazole binding at each Fe(III) heme site.

4. Discussion

The dependence of Hb spectroelectrochemistry on the presence of imidazole is an interesting example of active-site modification of the redox potential. One imidazole binds per Fe(III), and binds with very much lower affinity to Fe(II) [10]. The ligand field strength of imidazole is expected to stabilize the Fe(III) state and produce a low-spin (LS) electron configuration. This is consistent with the observed shift in $E°$ values to more negative potentials in the presence of imidazole (Table 1, and Figs. 2 and 3) and is consistent with studies of model Fe porphyrins [18,19] and myoglobin [10] in the presence of imidazole.

When H_2O is replaced by imidazole as an active-site ligand in metHb, the redox behavior of HbA_0 does not follow the behavior predicted by the two-state model. This is illustrated in Fig. 4, which is a plot of the maximum observed n value, n_{max}, as a function of the redox potential $E°$, for HbA_0, Hb Trout I, HbCPA and horse Mb in the presence of various heterotropic ligands and imidazole. The solid data points in Fig. 4 fall on a parabolic curve with a maximum n_{max} value of about 2, which occurs at a $E°$ of -100 mV (vs. Ag/AgCl).

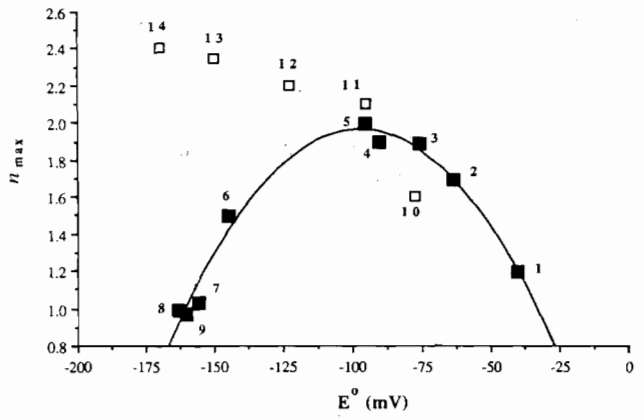

Fig. 4. Plot of n_{max} as a function of $E°$ (vs. Ag/AgCl) for various hemoglobins with H_2O as the homotropic ligand (filled symbols) and HbA_0 with varying concentrations of imidazole as the homotropic ligand (open symbols). Line through filled data points is a best fit polynomial curve. Data points are as follows: 1, HbA_0 in 0.05 M MOPS, 0.2 M $NaNO_3$ and IHP in excess; 2, HbA_0 in 0.05 M MOPS and 0.2 M $NaNO_3$; 3, Hb Trout I in 0.05 M MOPS and 0.2 M $NaNO_3$; 4, HbA_0 in 0.2 M MOPS; 5, HbA_0 in 0.05 M MOPS; 6, HbCPA in 0.05 M MOPS, 0.2 M $NaNO_3$ and IHP in excess; 7, HbCPA in 0.05 M MOPS and 0.2 M $NaNO_3$; 8, HbCPA in 0.2 M MOPS; 9, horse Mb in 0.05 M MOPS and 0.2 M $NaNO_3$; 10–14, 0.237 mM HbA_0 in 0.05 M MOPS and 0.2 M $NaNO_3$ with [imidazole] = 10, 0.82, 11, 10.4, 12, 23.2, 13, 52.3, 14, 104 mM. All data at pH 7.1 as shown in Table 1; data points 3–9 from Ref. [9].

The trend exhibited by these solid data points is consistent with the two state R↔T model, which is illustrated by the four-fold equilibrium in Eq. (3) (where $Hb(II)_R$ and $Hb(II)_T$ represent deoxyhemoglobin in the R and T state and $Hb(III)_R$ and $Hb(III)_T$ represent methemoglobin in the R and T state). Maximum co-

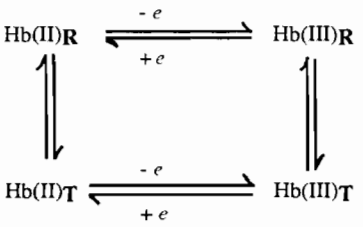

(3)

operativity, as expressed by a maximum n_{max} value, is found for HbA_0 in the absence of a heterotropic effector. Addition of a heterotropic effector typically stabilizes the T state, and shifts the redox potential positive and decreases cooperativity. This is illustrated in the right-hand side of Fig. 4. R state stabilization, which occurs in HbCPA and horse Mb, results in a decrease in redox potential and cooperativity, as illustrated in the left side of Fig. 4. The data points for HbA_0 in the presence of varying concentrations of imidazole are represented in Fig. 4 by open squares. Clearly the HbA_0/imidazole system does not follow the $n_{max}/E°$ trend established by various hemoglobins in the presence of heterotropic effectors.

The presence of imidazole in the system complicates the four-fold equilibrium as described in Eq. (3) by adding a new equilibrium: a spin state equilibrium of high-spin Fe(II) to low-spin Fe(III). The equilibrium in Eq. (4) is consistent with the results in Table 1 where H_2O is the only homotropic ligand, while the equilibrium in Eq. (5) is consistent with the results obtained in the presence of imidazole. The change in spin state in Eq. (5) complicates the two-state model and causes changes that are not predictable in terms

$$\underset{\text{high-spin}}{Hb(II)} + 4H_2O \longleftrightarrow \underset{\text{high-spin}}{Hb(III)H_2O} + 4e^- \quad (4)$$

$$\underset{\text{high-spin}}{Hb(II)} + 4Imid \longleftrightarrow \underset{\text{low-spin}}{Hb(III)Imid} + 4e^- \quad (5)$$

of the R↔T equilibrium shown in Eq. (3) alone. The ΔE_n values for HbA_0 in the presence of imidazole are consistent with stabilization of the T state [9], yet the $E°$ values are in the range expected when the R state is stabilized (as illustrated in Fig. 2). This behavior can best be explained by a process in which $E°$ is altered in the presence of imidazole by a mechanism that is independent of the R↔T equilibrium.

If the R↔T equilibrium is responsible for cooperativity in hemoglobins, and n_{max} is a measure of the cooperativity, then we would expect that the R↔T

equilibrium would not be affected by adding imidazole if the n_{max} value remained constant. We see in Fig. 3 (inset) that the n_{max} value increases to about 2.4, then levels off as the $E°$ continues to shift to negative. This trend is also evident in Fig. 4. This behavior is the result of additional electron density at the Fe porphyrin when imidazole is bound, stabilizing the Fe(III) and shifting the $E°$ value to negative.

It has been shown that there are two modes of allosteric regulation in the electron transfer process. Heterotropic and homotropic influences that reflect changes in the quaternary equilibrium between R and T states can be described using the two-state model of Monod, Wyman, and Changeux [7]. Active-site influences that act independently of this quaternary conformational shift must be described by an additional equilibrium not predicted in the two-state model. This is exemplified by the Hb–imidazole interactions herein reported that give rise to an additional equilibrium (Eq. (5)).

Perutz et al. have observed a lack of cooperativity for N_3^- and CN^- binding to metHb in the presence and absence of IHP [20]. Since both N_3^- and CN^- shift the spin state equilibrium for metHb to low-spin [11,12,21], one must conclude from this lack of cooperativity that a change in the spin state of the Fe center of HbA_0 does not constitute a change in quaternary structure. Likewise, it has been observed by paramagnetic resonance that adding IHP to HbN_3 or HbCN does not influence the spin state of the Fe center to a significant extent (<5%) [11]. These studies show that the high-spin to low-spin transition (HS/LS) and the R↔T equilibrium are independent of one another, and that a spin state change does not necessitate a quaternary structural change. Kelleher has recently discussed the issue of a linkage of the R↔T equilibrium and the HS/LS transition [21]. He first makes it clear that the HS/LS states are in equilibrium with one another, and that HbCN and HbN_3 are at the low-spin extreme of the equilibrium. Thus, addition of an allosteric effector such as IHP has little effect on this equilibrium since the HS/LS equilibrium starts at the LS extreme.

These observations are consistent with our spectroelectrochemical results which show that imidazole alters the redox potential by shifting the HS/LS equilibrium, but has little or no influence on the R↔T equilibrium, as indicated by the values of ΔE_n (15–30 mV; Table 1) which are indicative of T state hemoglobins [9]. This also explains the lack of consistency of the imidazole data with the parabolic shaped curve of Fig. 4. The n values remain constant while the redox potential becomes more negative with increasing [imidazole] (see Fig. 3). This leads us to propose an additional axis to the four-fold equilibrium (Eq. (3)) which is illustrated in Fig. 5. In this scheme the x-axis represents the redox

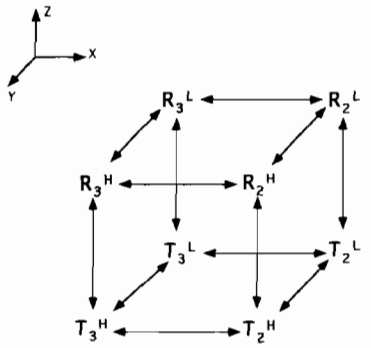

Fig. 5. Scheme illustrating the oxidation/reduction, R state/T state, and high-spin/low-spin equilibria. Symbols: R and T represent the R and T quaternary states for hemoglobin; superscript H and L represent high-spin and low-spin Fe, respectively; subscript 2 and 3 represent deoxy(Fe(II)) and met(Fe(III)) hemoglobin. See text.

equilibrium, the y-axis represents the HS/LS equilibrium, and the z-axis represents the R↔T equilibrium. Our spectroelectrochemical data are consistent with this model for the case of HbA_0 oxidation/reduction in the presence of imidazole. Thus, we conclude that the HS/LS equilibrium can be independent of the R↔T equilibrium, making the MWC model inadequate to describe the spectroelectrochemical data we obtain for HbA_0 oxidation/reduction in the presence of imidazole.

Acknowledgements

Financial support was provided by the Arts and Sciences Research Council and NIH Center Grant ESO 1908. We gratefully acknowledge Dr Fethi Bedioui, Ecole Nationale Supérieure de Chimie de Paris for helpful discussions.

References

[1] E. Di Cera (ed.), *Biophys. Chem., 37* (1990) 14–411 (J. Wyman Special Edition).
[2] J.M. Rifkind, *Adv. Inorg. Chem., 7* (1987) 155.
[3] M.F. Perutz, G. Fermi, B. Luisi, B. Shaana and R.C. Liddington, *Acc. Chem. Res., 20* (1987) 309.
[4] B. Luisi, B. Liddington, G. Fermi and N. Shibayama, *J. Mol. Biol., 214* (1990) 7.
[5] A. Levy, V.S. Sharma, L. Zhang and J.M. Rifkind, *Biophys. J., 61* (1992) 750.
[6] M.F. Perutz, *Trends Biol. Sci., 14* (1989) 42.
[7] J. Monod, J. Wyman and J.-P. Changeux, *J. Mol. Biol., 12* (1965) 88.
[8] J. Baldwin and C. Chothia, *J. Mol. Biol., 129* (1979) 175.
[9] K.M. Faulkner, C. Bonaventura and A.L. Crumbliss, *J. Biol. Chem.*, submitted for publication.
[10] E. Antonini and M. Brunori, *Hemoglobin and Myoglobin in their Reaction with Ligands*, North-Holland, Amsterdam, 1971.
[11] J.S. Philo and U. Dreyer, *Biochemistry, 24* (1984) 2985.
[12] J. Beetlestone and P. George, *Biochemistry, 3* (1964) 707.
[13] C. Bonaventura and J. Bonaventura, *Am. Zool., 20* (1980) 131.

[14] R.A. Greenwald (ed.), *CRC Handbook of Methods for Oxygen Radical Research,* CRC, Boca Raton, FL, 1985, pp. 137–141.
[15] M.L. Furst and R.A. Durst, *Anal. Chim. Acta, 140* (1982) 1.
[16] E.W. Kristensen, D.H. Igo, R.C. Elder and W.R. Heineman, *J. Electroanal. Chem., 30* (1991) 61.
[17] M.M. Rubin and J.-P. Changeux, *J. Mol. Biol., 21* (1966) 265.
[18] K.M. Kadish, A. Tabard, W. Lee, Y.H. Liu, C. Ratti and R. Guilard, *Inorg. Chem., 30* (1991) 1542.
[19] D. Lexa, M. Momenteau, J. Mispelter and J.M. Lhoste, *Bioelectrochem. Bioenerg., 1* (1974) 108.
[20] M.F. Perutz, A.R. Fersht, S.R. Simon and G.C.K. Roberts, *Biochemistry, 13* (1974) 2174.
[21] M.J. Kelleher, *Acc. Chem. Res., 26* (1993) 154.